Supplementary Material for:

Molecular basis for the substrate stereoselectivity in Tryptophan Dioxygenase

Luciana Capece[1], Ariel Lewis-Ballester[2], Marcelo A. Marti[1, 3], Dario A. Estrin[1*], and Syun-Ru Yeh[2*]

[1]*Departamento de Química Inorgánica, Analítica y Química Física/ INQUIMAE-CONICET Facultad de Ciencias Exactas y Naturales, Universidad de Buenos Aires, Ciudad Universitaria, Pabellón 2, Buenos Aires, C1428EHA, Argentina,* [2]*Department of Physiology and Biophysics, Albert Einstein College of Medicine, 1300 Morris Park Avenue, Bronx, New York 10461 USA.* [3]*Departamento de Química Biológica, Facultad de Ciencias Exactas y Naturales, Universidad de Buenos Aires, Ciudad Universitaria, Pabellón 2, Buenos Aires, C1428EHA, Argentina.*

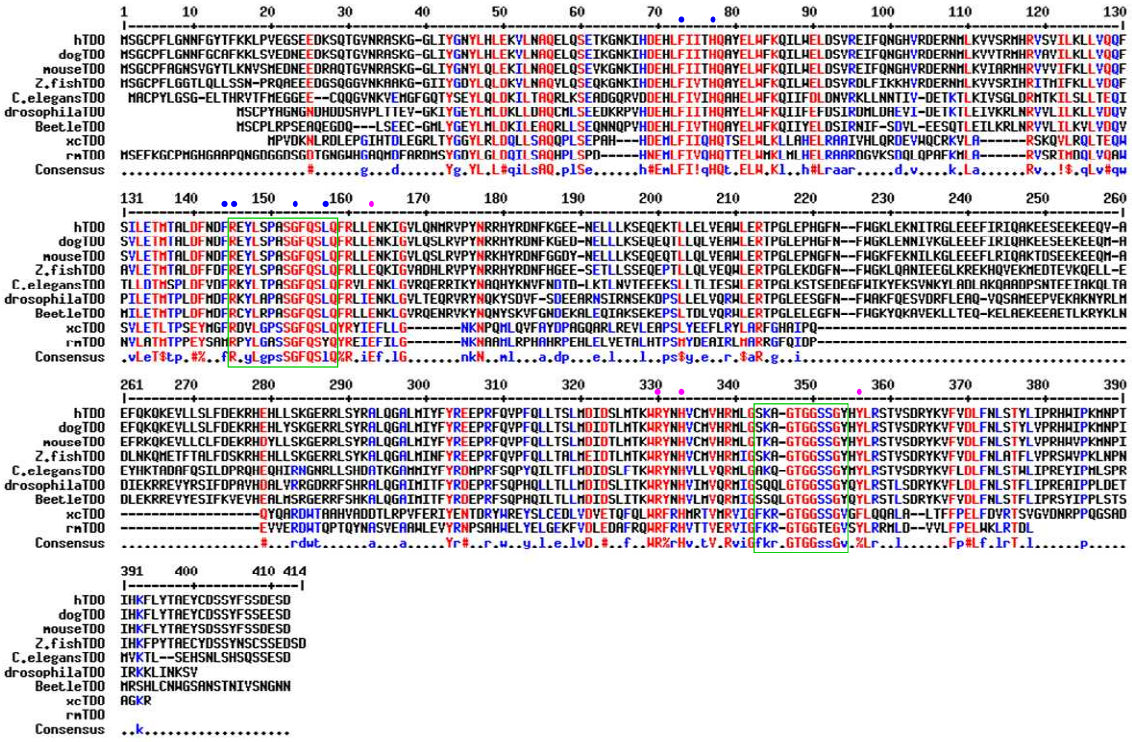

Figure S1. Sequence alignment of TDO from various species. The accession code associated with each species is: human (P48775), dog (XP_532700), mouse (NP_064295), zebra fish (NP_956150), *C. elegans* (Q09474), fruit fly (P20351), red flour beetle (NP_001034499), *R. metallidurians* (Q1LK00), and *X. campestris* (B0RMW5). Blue and magenta dots labeled on the top of the sequences indicate the conserved distal and proximal amino acids in the active site. The green boxes indicate the location of the two critical loops ($loop_{117\text{-}130}$ and $loop_{250\text{-}260}$) involved in the conformational changes in the L-Trp-O_2 complexes and Ferryl/indole 2,3-epoxide intermediates of xcTDO (see Text).

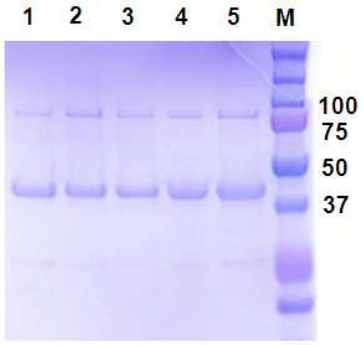

Figure S2. SDS-PAGE data showing the purity of the T342A mutant of hTDO. The lane "M" corresponds to molecular markers (BioRad). Molecular weights are given in kDa on the right. The line with lower intensity around ~80 kDa is attributed to the dimeric form of the enzyme.

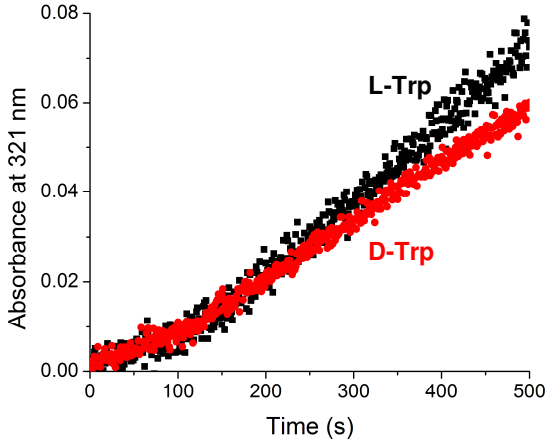

Figure S3. NFK formation as function of time during the reaction of the T342A mutant of hTDO with L-Trp (black trace) and D-Trp (red trace). The concentration of Trp was 8 mM.

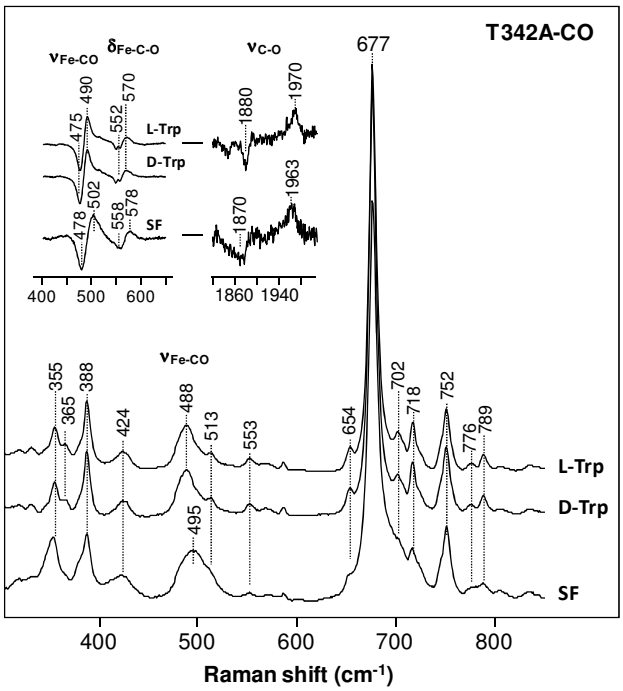

Figure S4. Resonance Raman Spectra of the CO-complex of the T342A mutant in the absence (SF) and presence of L-Trp or D-Trp. The insert shows the $\nu_{Fe\text{-}CO}$, $\delta_{Fe\text{-}C\text{-}O}$ and $\nu_{C\text{-}O}$ modes identified in the corresponding ^{12}CO-^{13}CO difference spectra.

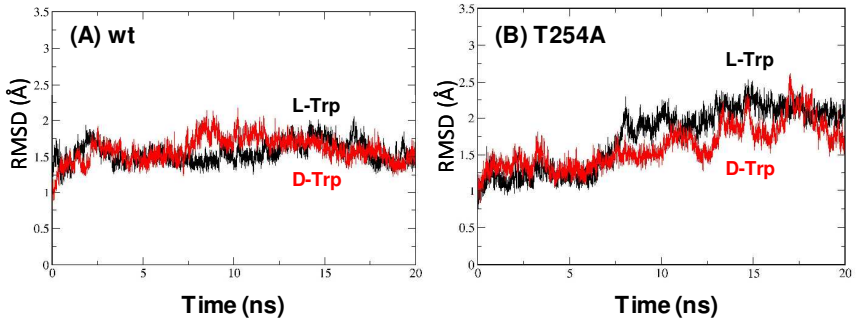

Figure S5. Root-mean-square-deviation (RMSD) from the initial structure of the Trp-bound wild type (A) and T254A mutant (B) of xcTDO as a function of MD simulation time. The black and red traces correspond to the complex with L and D-isomer, respectively.

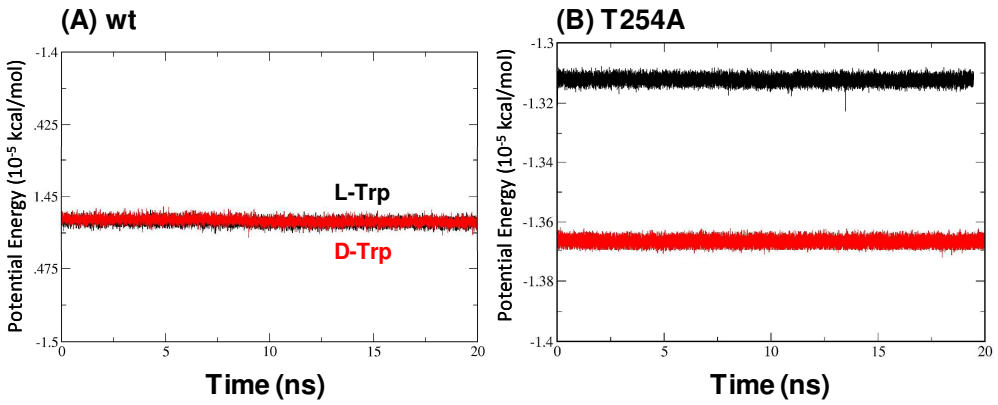

Figure S6. Potential energy of the Trp-bound wild type (A) and T254A mutant (B) of xcTDO as a function of MD simulation time. The black and red traces correspond to the complex with L and D-isomer, respectively.

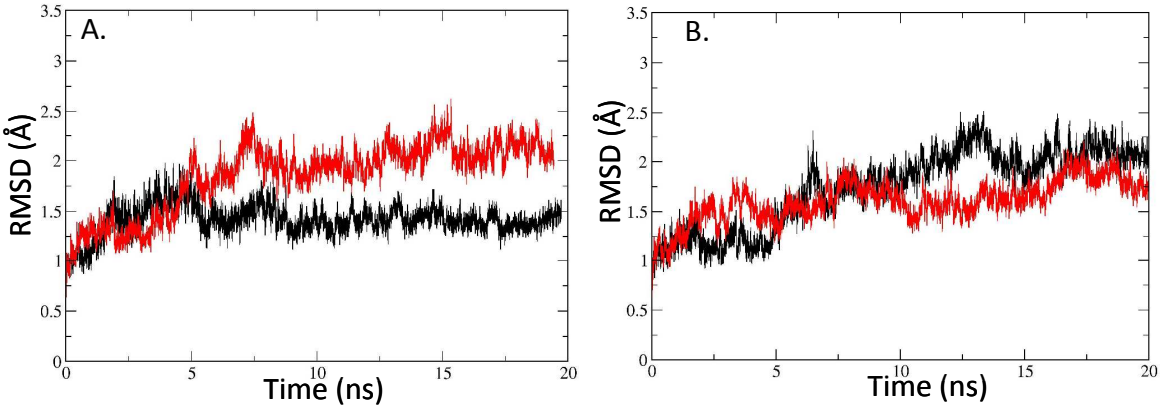

Figure S7. Root-mean-square-deviation (RMSD) from the initial structure of the ferryl/indole 2,3-epoxide intermediate of the wild type (A) and T254A mutant (B) of xcTDO as function of MD simulation time. The black and red traces correspond to the complex with L and D-isomer, respectively.

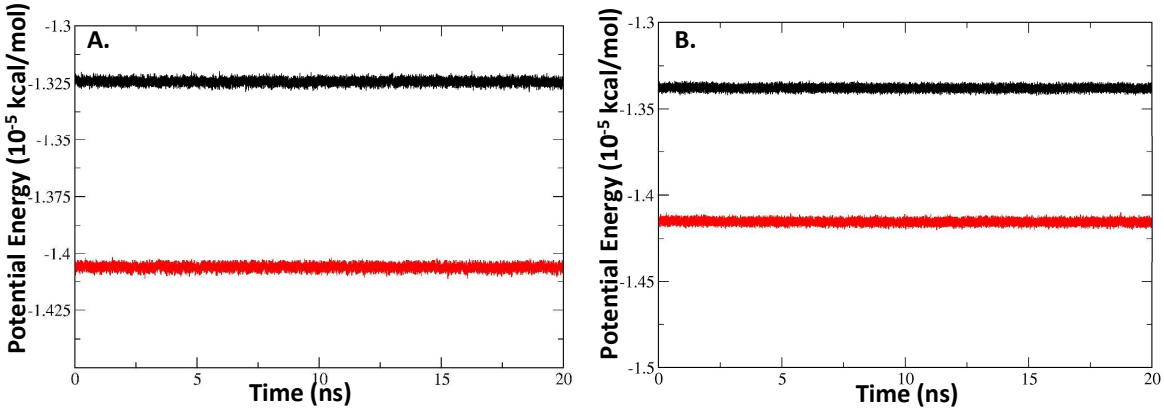

Figure S8. Potential energy of the ferryl/indole 2,3-epoxide intermediate of the wild type (A) and T254A mutant (B) of xcTDO as a function of MD simulation time. The black and red traces correspond to the complex with L and D-isomer, respectively.

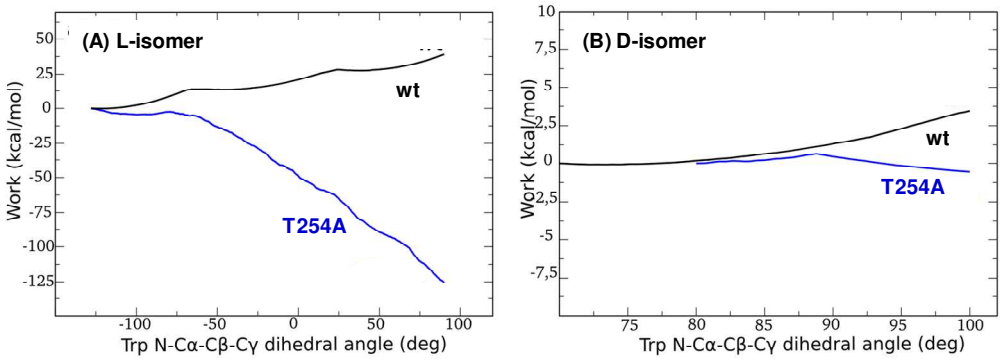

Figure S9. Calculated work for the transformation from the closed to open conformation in the ferry/indole 2,3-epoxide intermediate of the wild type and T254A mutant of xcTDO. Results for L and D-isomers are shown in panels (A) and (B), respectively. The black and blue traces were obtained from the wild type and T254A mutant of xcTDO, respectively. In all four cases, the calculation was performed using the Trp-N-C_α-C_β-C_γ dihedral angle as the coordinate for the transition, as explained in the Materials and Methods section. For each structure, the starting value of the reaction coordinate corresponds to the equilibrium position in the closed conformation.